MRU Cardington Technical Note No. 7

An investigation into the validity of the temperature fluctuations and heat flux relations for several stability conditions with a sonic anemometer

by

Miss.J.L. Jones

July 1991

Met. Office Research Unit
RAF Cardington
Shortstown
Beds, MK42 0TH

MRU CARDINGTON

Note

This paper has not been published and PMetO(Cardington) should be consulted before quoting from it.

MRU Cardington Technical Note No. 7

An investigation into the validity of the temperature fluctuations and heat flux relations for several stability conditions with a sonic anemometer

by

Miss.J.L.Jones

July 1991

Met. Office Research Unit
RAF Cardington
Shortstown
Beds, MK42 0TH

Note

This paper has not been published and PMetO(Cardington) should be consulted before quoting from it.

An investigation into the validity of the temperature fluctuations and heat flux relations for several stability conditions with a sonic anemometer

Miss. J. L. Jones

July 1991

Abstract

The theoretical relations for sonic temperature fluctuations and heat flux were derived and investigated for stable, near neutral and unstable surface-layer conditions. The parameters required were measured with a sonic anemometer, platinum resistance thermometer and an Ophir IR-2000 hygrometer. The investigation undertaken determined which of the relation terms were significant, enabling the degree of departure from the theoretical relations for each specific stability condition to be identified.

1 Introduction

Measurement of sonic temperature fluctuations are in general not equal to platinum resistance temperature fluctuations (σT_s and σT respectively), similarly for sonic temperature flux ($\overline{w'T's}$) and PRT temperature flux ($\overline{w'T'}$). This report underlies the degree of departure from the above case for each stability condition by the use of the theoretical relations established by Kaimal and Businger, 1963 and the first estimate of the error terms deduced by Kaimal, 1969. Determination of these required direct observation of all the correction terms contained within the relations.

The stability ranges studied were of three types:- stable, nearly neutral and unstable conditions. Stable conditions, involved weak, sporadic turbulence characterised by

statically stable air causing short bursts of turbulence. Whereas, nearly neutral stability had a turbulence intensity equal in all directions having been formed from unstable turbulence decay as a result of cold air advection. Finally, unstable conditions involved convectively driven turbulence where sources of heat transfer included those from a warm ground surface, which create thermals of warm air rising from the ground layer and radiative cooling from cloud layer tops, creating sinking cold air thermals.

Measurement of the three vertical turbulent fluxes; heat, momentum and moisture were made. This was of value since the work undertaken by Kaimal, 1969 indicated the result that the sonic derived temperature was affected by humidity and velocity fluctuations and that the sonic derived temperature flux was affected by humidity and momentum fluxes.

The various aspects of the experiment have been subdivided into the subsequent sections: sonic anemometer theory (section 2); instrumental set up and description (section 3); experimental data analysis (section 4); conclusions (section 5).

2 Theory

For sonic anemometer temperature calculation temperature measurements with a sonic anemometer turbulence probe such as that below, Figure 1, involve the transmittance of ultrasonic pluses back and forth between transducers (Figure 2).

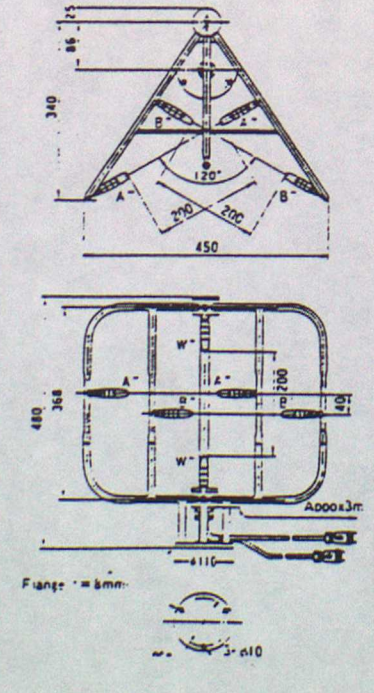

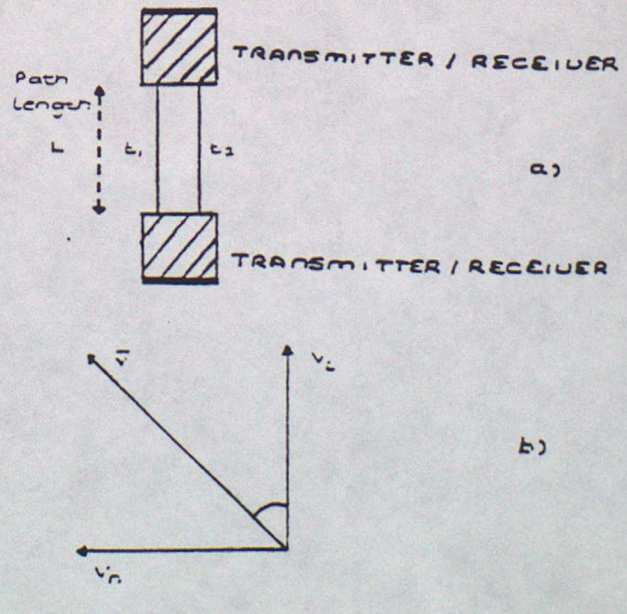

Figure 1: TR-61A Turbulence Probe

Figure 2: a) Transducer Sketch

b) Velocity vector diagram: $\overline{v}$– mean wind at d to transducer path

v_L – *ver* component along path

v_n – *ver* component normal to path

Transit times for pulses emitted by one transducer and received by its partner, given by equation (1).

$$t_1 = \frac{L}{c\cos\alpha + v_L} \quad , t_2 = \frac{L}{c\cos\alpha - v_L}, \tag{1}$$

where c = speed of sound

$\alpha = \sin^{-1}(v_n/c)$

By the addition of the reciprocals of the transit times a relation in terms of the speed of sound is found, equation (2)

$$c = \frac{L}{2\cos\alpha}\left(\frac{1}{t_1} + \frac{1}{t_2}\right) \tag{2}$$

The sound velocity given by (3) shows it to be temperature dependent

$$c^2 = \gamma RT(1 + 0 \cdot 61q) \tag{3}$$

where γ R $= 403m^2s^{-2}k^{-1}$

T = temperature

q = humidity (specific)

The sonic anemometer output, T_s, can then be obtained: equation (4) as shown in Appendix 1.

$$T_s = \frac{L^2}{4\gamma R}\left(\frac{1}{t_1} + \frac{1}{t_2}\right)^2 \tag{4}$$

Temperature, humidity, angle α and speed of sound can be separated into mean and fluctuating parts (denoted by overbars and primes respectively) as shown by (5)

$$T = \overline{T} + T' \tag{5}$$

$$q = \overline{q} + q' \tag{6}$$

$$\cos\alpha = \overline{\cos\alpha} + \cos\alpha' \tag{7}$$

$$c = \overline{c} + c' \tag{8}$$

A 1st-order Taylors expansion and subsequent substitution produced the following important results.

mean sonic temperature, $\overline{T_s}$:

$$\overline{T_s} = \overline{T}(1 + 0 \cdot 61\overline{q}) \tag{9}$$

fluctuating part of sonic temperature, T_s' :

$$T_s' = T' + 0 \cdot 61 q' \overline{T} - \frac{2\overline{T}}{c^2}\overline{V_n} V_n' \tag{10}$$

sonic temperature variance

$$\sigma^2 T_s \equiv \overline{T_s'^2} = \sigma_T^2 + 1 \cdot 22\overline{T}\ \overline{q'T'} + (0 \cdot 61)^2 \overline{T}^2 \sigma_q^2$$

$$+ \frac{4\overline{T}^2\overline{u}^2}{(\overline{c^2})^2}\sigma_u^2 - \frac{4}{\overline{c^2}}\overline{T}\ \overline{u}\ \overline{u'T'} - \frac{2 \cdot 44}{\overline{c^2}}\overline{T}^2\overline{u}\ \overline{u'q'} \tag{11}$$

correlation of T_s with vertical velocity w:

$$\overline{w'\,T_s'} = \overline{w'T'} + 0 \cdot 61\overline{T}\ \overline{w'q'} - \frac{2}{\overline{c^2}}\overline{T}\,\overline{u}\,\overline{u'w'} \tag{12}$$

The derivations of (9) to (13) are contained within the Appendixes with the analysis of (12) and (13) given in section 4.

3 Instrumental Set-up

The field experiment was conducted with the use of a meteorological mast, at the Meteorological Office Research Unit, Cardington. The surroundings of the mast consisted of flat grassland a distance away from obstacles, in the form of buildings. Several instruments were employed during the experiment which are described below.

A three-dimensional Kaijo-Denki sonic anemometer, model DAT-300 was used. A directional head sensor (model TR-61A) with a vertical sound path and two horizontal sound paths with 120° intersecting angle produced measurements of the three velocity components u, v, w at a maximum frequency response of 20Hz. The manufacturer quoted accuracy being $\pm 1\%$ and of resolution 0·5 cms^{-1}. The length of each sound path was 0·2m with the sound transducers diameter about 15mm. The wind velocity range started from zero to a maximum of 30 m/s.

Temperature fluctuations were measured by two methods. Firstly, by the installation of a platinum resistance thermometer consisting of a 25μm diameter helical coil of 150Ω nominal resistance. This was mounted within the measuring volume of the sonic anemometer attached to the frame. And, secondly by the use of the ultrasonic anemometer speed of sound deductions from sonic flight path times between transducers. The sonic anemometer with its thermometric capability had a zero inertia time along with a response time of 0·05 sec. The thermometer design prevented radiant heat effects with the advantage of a zero thermal capacity.

Atmospheric humidity fluctuations required the use of an Ophir IR-2000 hygrometer (dual wavelength) capable of fast response measurements. The dual wavelengths used were a $2 \cdot 50\mu$m reference channel and a $2{\cdot}60\mu$m absorption channel - use of which avoided a weak CO_2 absorption band.

Extinction of aerosols and water droplets over the 2·50 - 2·60 μm frequency band was expected to vary only slightly and be much less in magnitude than the vapour absorption.

The construction of the instrument allowed both the source detector and electronics to be housed in a cylindrical head. Entry and exit of radiation through the IR hygrometer took place through windows in its lower face with reflection occuring at a mounted mirror situated within the lower end of the open frame above a shielded temperature sensor. The quoted manufacturers path length was given as 56·2cm with communication via a RS-422 serial line - cable lengths up to 300m - and a unit indicator module (U.I.M.). The UIM facilitated interfacing to a selection of data logging systems.

Calibrated data at 1Hz for absolute, dewpoint and relative humidity was available. Over the operational dewpoint range (-40°C to 40° C) the quoted accuracy and resolution were 1·0°C above 0 · 0°C to 1·5°C below 0·0°C and 0·2°C above 0·0°C to 1·0°C at -40°C respectively.

The whole array of turbulence instruments were mounted on a mast at a height of 12m with the sonic anemometer and IR hygrometer side by side. The centres of the working volumes of the two instruments had zero vertical and a horizontal separation of 1m. A remotely controlled rotator allowed the mount to be turned into a position so that it faced across the mean wind direction which effectively pointed the sonic anemometer into the wind.

The relatively bulky nature of the sonic anemometer and hygrometer, 0·5m maximum dimensions, meant that a separation of 1m was required between the recording instruments. This took into consideration minimisation of mutual flow distortion effects generated between the instruments, as well as the attempt to maintain correlation between both measurements. All the instruments analogue outputs were taken as inputs to one 12-bit A/D converter. This had a digitization rate of 20·76Hz. A recording rate of 10·38Hz was calculated by the averaging by 2 of the digitized data.

4 Results

This section discusses the verification and degree of correlation with relations (11) and (12) from the data observed, over the three stability ranges.

For the calculation of the variances and covariances the collected data were linearly detrended and the vertical components rotated so as to give zero mean lateral and vertical components.

The total experiment involved observations from several days, which produced a large quantity of data. During each day, data was recorded in runs of 2 hours duration after which the quantity of data was reduced by subdivision into 10 and 30 minute averaged sets for later analysis.

A means of determining which data groups falls into the respective stability conditions was done from the sign of the groups dimensionless value Z/L.

where Z - height above ground level.

L - Monin Obhukhov length; calculated from PRT temperatures.

Z/L varied greatly with the stability conditions.

For nearly neutral conditions Z/L is theoretically zero though for our case an experimental nominal band width, given below, was used to delimit such a stability.

$$-0 \cdot 025 \leq Z/L \leq 0 \cdot 025 \tag{13}$$

The sonic temperature variance $\sigma^2 T_s$ was first considered. A value for σts was obtained directly from the sonic anemometer output. This valve was related by means of equation (11), applicable in all stability conditions, to the humidity data of the hygrometer, wind velocity of the sonic anemometer and PRT temperature.

4.1 Variances

4.1.1 Stable

For measurements made under stable conditions it was found that all the terms on the right hand side of (11) were negligible except the first.

A term which produced a magnitude variation of less than 5% of the whole relation was assumed to have a negligible effect.

For stable conditions relation (11) can be reduced to

$$\sigma_{T_s} = \sigma_T \tag{14}$$

Relation (14) holds very well with the theoretically ideal linear correlation. On average σ_{T_s} was 2% greater than σ_T.

From the right hand side of equation (11) the σ_{T_s} correction terms were computed successfully, initially by the inclusion of the first term, as above. Then by increasing the number of terms one by one, in the approximation to be plotted against σ_{T_s}, until

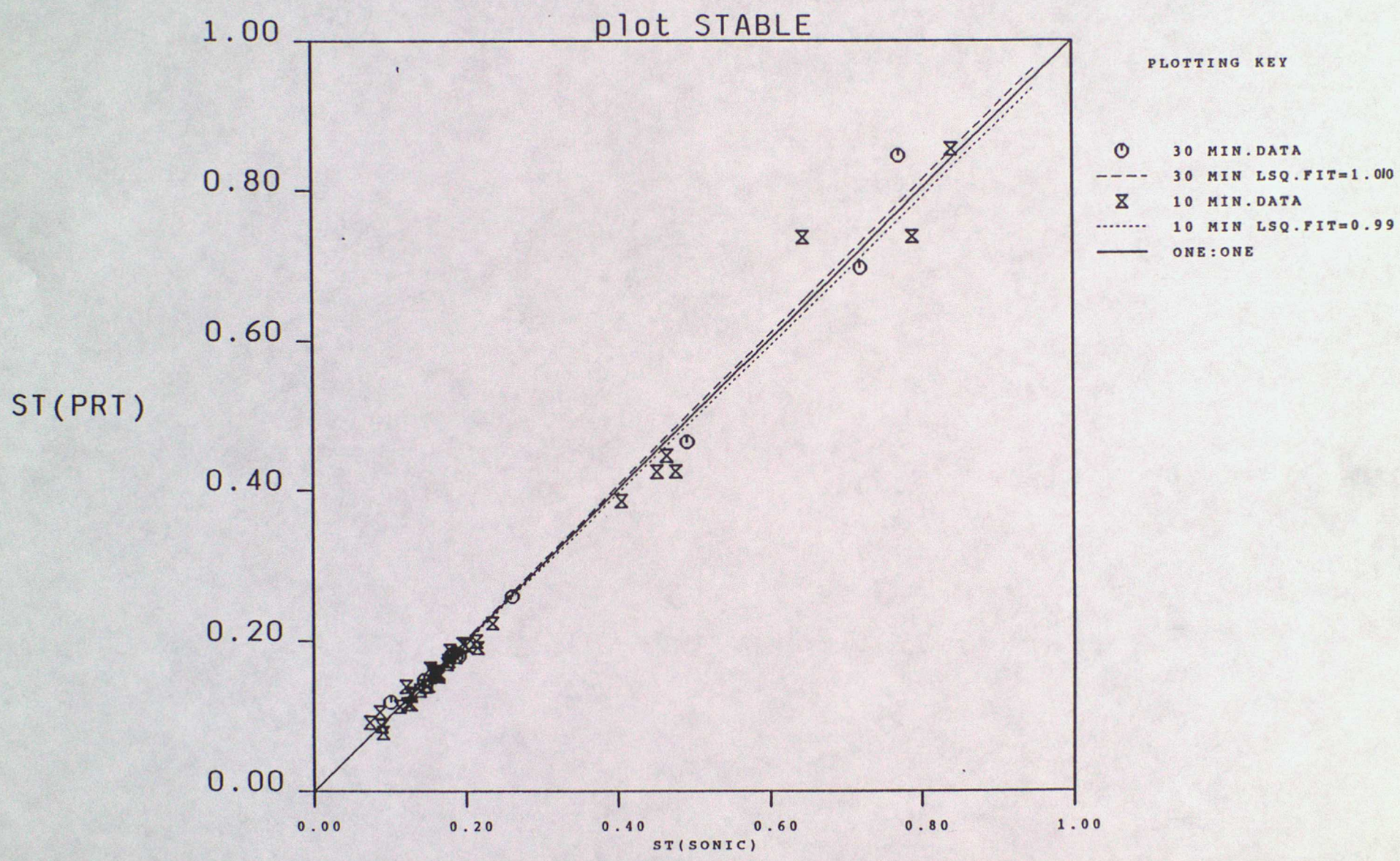
plot STABLE
1.00
0.80
0.60
0.40
0.20
0.00
ST(PRT)
0.00
0.20
0.40
0.60
0.80
1.00
ST(SONIC)
PLOTTING KEY
30 MIN.DATA
30 MIN LSQ.FIT=1.010
10 MIN.DATA
10 MIN LSQ.FIT=0.99
ONE:ONE

FIGURE 3

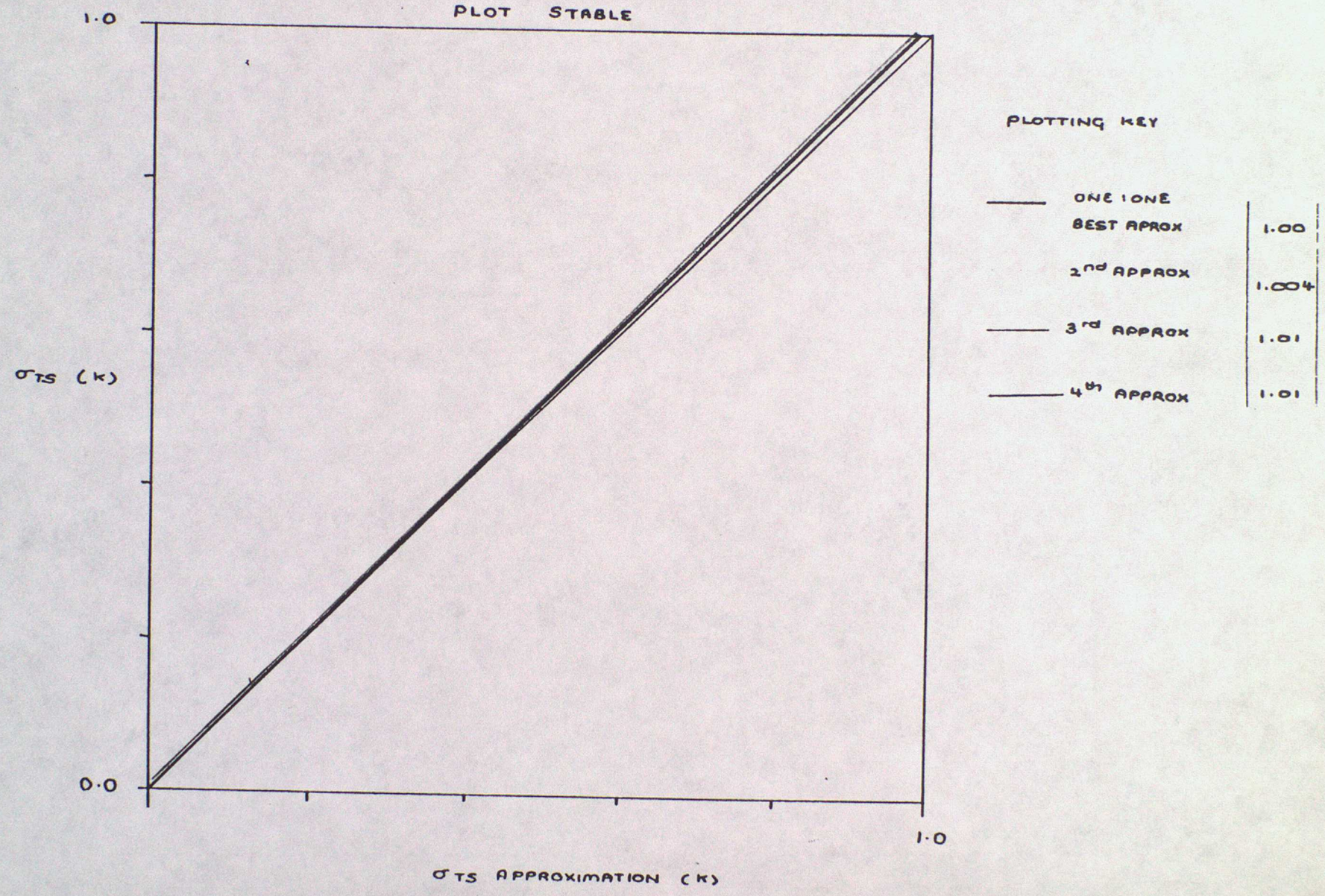
PLOT STABLE
1.0
0.0
σ_{TS} (K)
1.0
σ_{TS} APPROXIMATION (K)
PLOTTING KEY
ONE ! ONE
BEST APROX 1.00
2nd APPROX 1.004
3rd APPROX 1.01
4th APPROX 1.01

FIGURE 4

all six terms were included. The slopes given by the figures were obtained by a least squared fit line through the origin.

Analysis of increasing stable approximations showed similar slopes to those of the direct σ_{T_s}, σ_T relationship given by Figure 3, though there was a general variation of $\pm 1\%$ from perfect behaviour. Development of the successive approximations produced a decreasing slope trend, indicative of a worsening effect on the correlation. In an attempt to explain this effect a study of possible correlations between $\overline{q'T'}$, $\overline{u'T'}$ and $\overline{u'q'}$ from equation (11) was considered.

On observation of all the 3 individual terms it was found that there was no correlation between the parameters. Analysis of the relative magnitudes of all the terms other than σ_T^2 indicated that all the terms were small and could be termed negligible in comparison with the 97% contribution from σ_T. Correction terms though negligible in themselves with relative contributions of: 1% - term 2 and 5, 1·5% - term 3 and independent of term 4 and 6 manifest themselves in an accumulative manner. This gradual accumulation of small correction terms due to successive approximations lies consistent with the manner of the correlation deterioration given by Figure 4.

Relation (14) provided the best approximation from the data analysed indicating that fluctuations in sonic temperature readings were equivalent to those produced by a platinum resistance thermometer with the data spread of $\sigma_{T_s} \sim 2 \cdot 5$ spread σ_T.

4.1.2 Nearly neutral

For measurements taken during nearly neutral conditions, it was found that a more complicated relationship existed than that for stable data. Analysis of the data in the same manner as for stable conditions resulted in the conclusion that fluctuations in sonic temperature under neutral conditions follow the relationship below. Its verification if given by Figure 5.

$$\sigma_{T_s}^2 = \sigma_T^2 + 1 \cdot 22\overline{T}\ \overline{q'T^1} + (0 \cdot 61)^2 \overline{T}^2 \sigma^2 q + \frac{4\overline{T}^{\ 2}}{(\overline{c^2})}\ \overline{u}^2\, \sigma^2 u \qquad (15)$$

$$c - \frac{4\overline{T}}{\overline{c^2}} \overline{u} \overline{u'\, T'}$$

For a rough approximation the equation below is sufficient for and calculations,

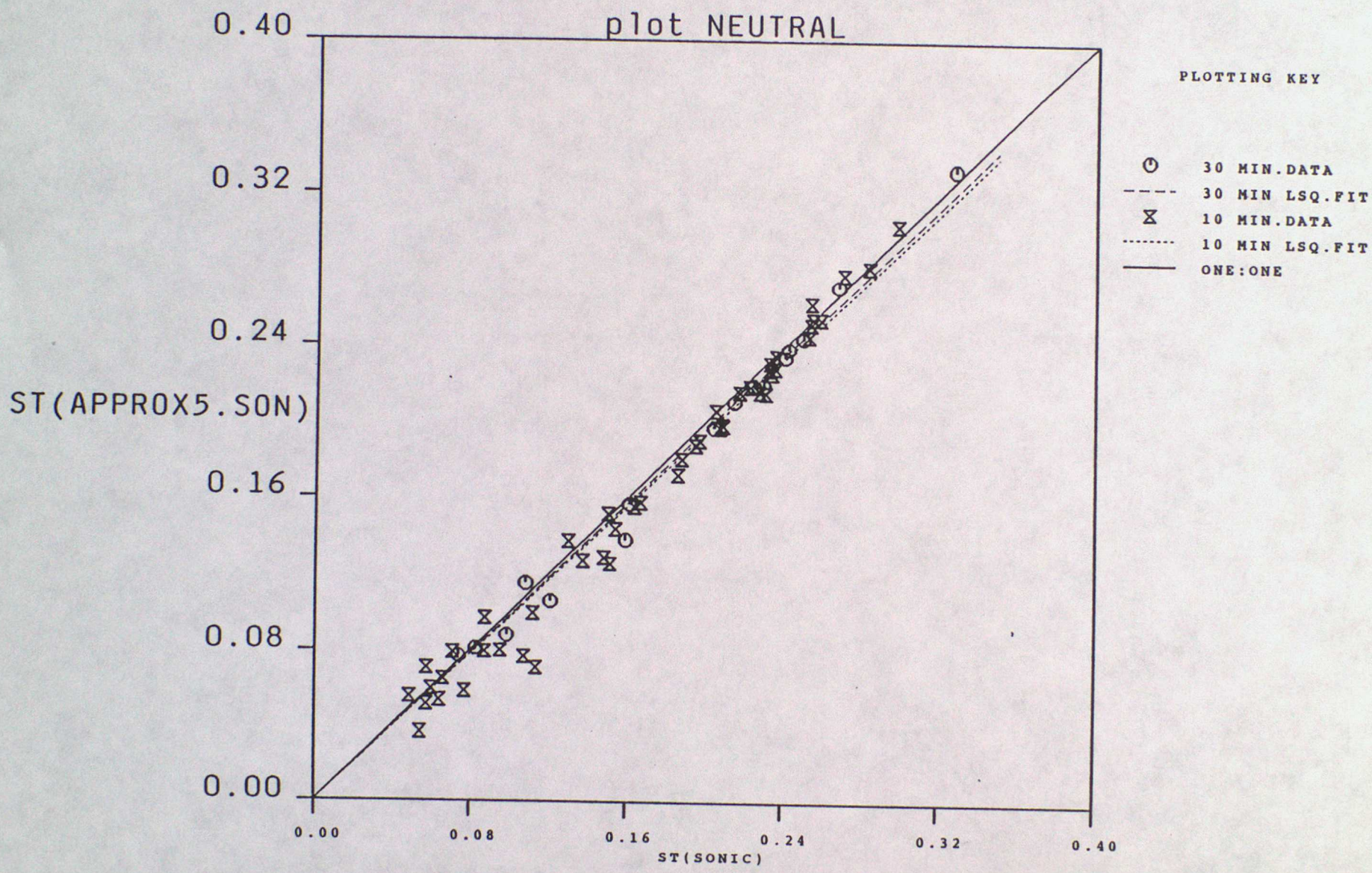
plot NEUTRAL
0.40
0.32
0.24
0.16
0.08
0.00
ST(APPROX5.SON)
0.00
0.08
0.16
0.24
0.32
0.40
ST(SONIC)
PLOTTING KEY
30 MIN.DATA
30 MIN LSQ.FIT
10 MIN.DATA
10 MIN LSQ.FIT
ONE:ONE

FIGURE 5

shown in Figure 6.

$$\sigma^2_{T_s} = \sigma^2_T + 1 \cdot 22\,\overline{T}\;\overline{q'T'} \tag{16}$$

where σ^2_T contributes relative magnitude of 30% and second correction term 29% to $\sigma^2_{T_s}$. Relation (16) has a data spread equivalent to 80% spread of $\sigma^2_{T_s}$.

Overall, relation (15) provided the best approximation to $\sigma^2_{T_s}$ under near neutral stability with a departure of 3% from the ideal one: one relationship compared with that of 9% for equation (16).

From the improved approximation (15) which well approximated linear behaviour, it was found that $\sigma^2_T > \sigma^2_{T_s}$.

Figure 7 gives the analysis of increasing approximations for nearly neutral data.

The addition of increasing correction terms to approximations, up to the 4th, saw a gradual worsening of the correlation though a significant improvement was seen for relation (15) by the addition of term 5. Though term 4, contained σ^2_u which would have been assumed to be of negligible effect, its omittance produced a change in the linear plot of Figure 5 by +6% causing a subsequent reversal so that $\sigma_{T_s} > \sigma_T$

As a contrast between stable an neutral conditions; during nearly neutral stability the relative magnitude of σ^2_T was much less equivalently $\frac{2}{3}$ less than that for stable conditions. This was compensated by the magnitude of terms 2 and 3 ($\overline{q'T'}$ and σ^2_q) which had a greater relative importance in this stability range.

A study of the decline in the slope accuracy by the investigation of possible relationships between $\overline{q'T'}$, $\overline{u'T'}$ and $\overline{u'q'}$ resulted in a relationship between $\overline{u'T'}$ and $\overline{q'T'}$, Figure 8. The linear relationship holds well though as $\overline{q'T'}$ and $\overline{u'T'}$ increased the spread of the data similarly increased. As with all the stability data observed, there was only a small variation , averaged at 4%, between 10 and 30 minute averaged data.

Under neutral conditions the correlation of Figure 8 was distinct. From a slope of 0·44 and substitution to (11) the following relationship below was formed, Figure 9.

$$\sigma^2 T_s = \sigma^2_T + 3\,\overline{T}\;\overline{q'T'} + 4\frac{\overline{T}^2}{\overline{(c^2)}}\,\overline{u}^{\,2}\sigma^2 u \tag{17}$$

The gradual deterioration and then sudden improvement of the gradient found from

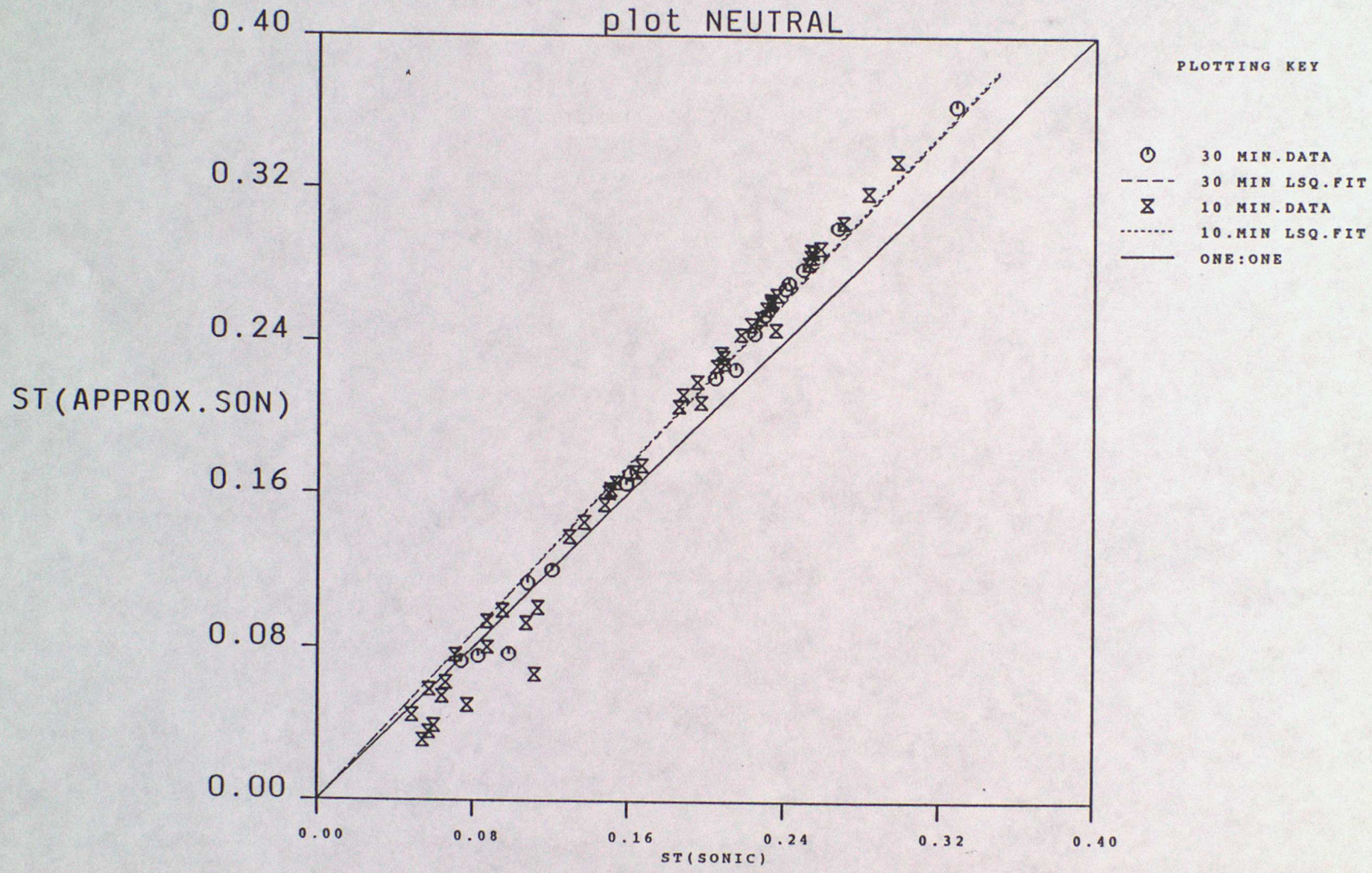
plot NEUTRAL
0.40
0.32
0.24
0.16
0.08
0.00
ST(APPROX.SON)
0.00
0.08
0.16
0.24
0.32
0.40
ST(SONIC)
PLOTTING KEY
30 MIN.DATA
30 MIN LSQ.FIT
10 MIN.DATA
10.MIN LSQ.FIT
ONE:ONE

FIGURE 8

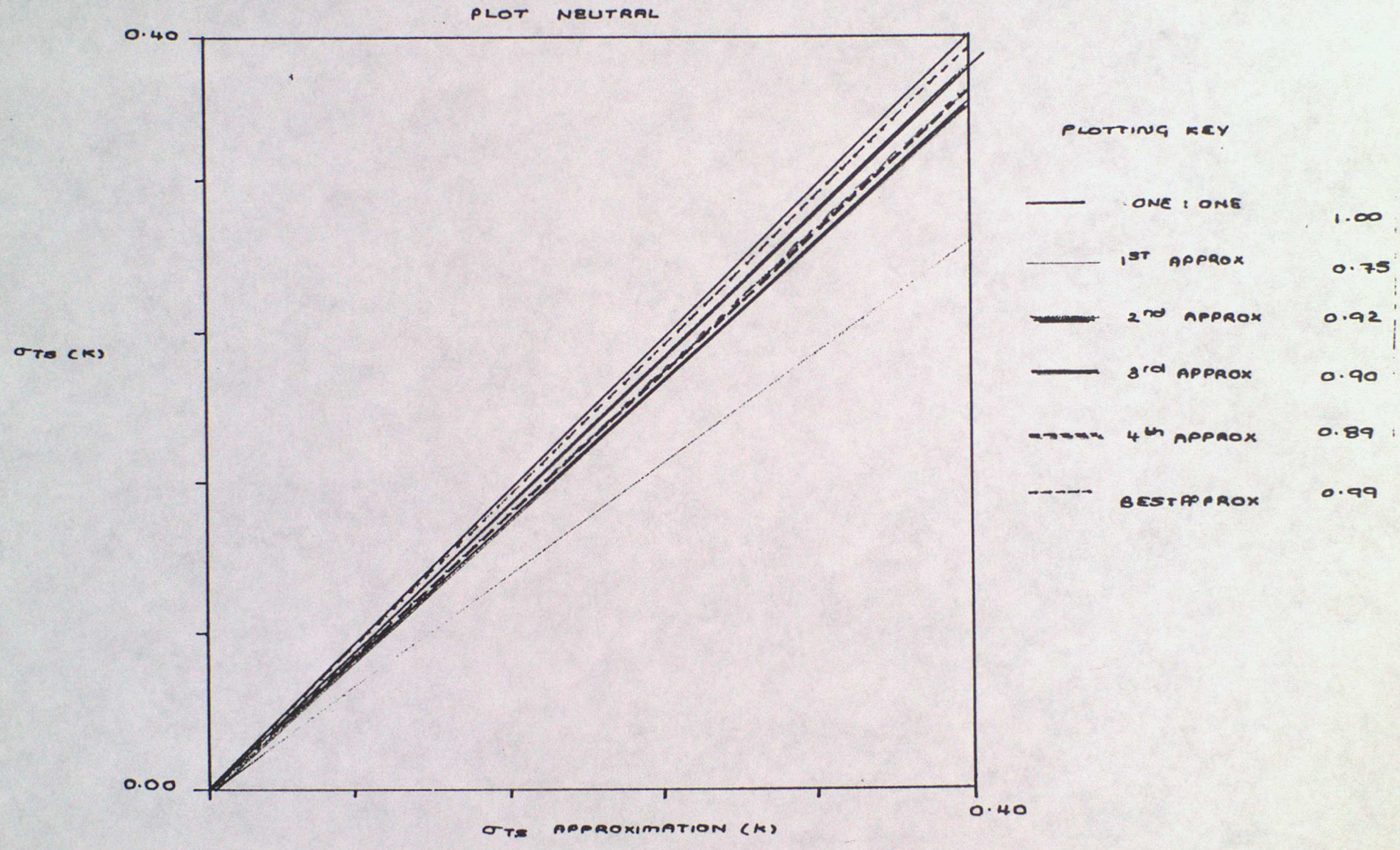
PLOT NEUTRAL
0·40
0.00
σTs (K)
σTs APPROXIMATION (K)
0·40
PLOTTING KEY
ONE : ONE
1·00
1ST APPROX
0·75
2nd APPROX
0·92
3rd APPROX
0·90
4th APPROX
0·89
BEST APPROX
0·99

FIGURE 7

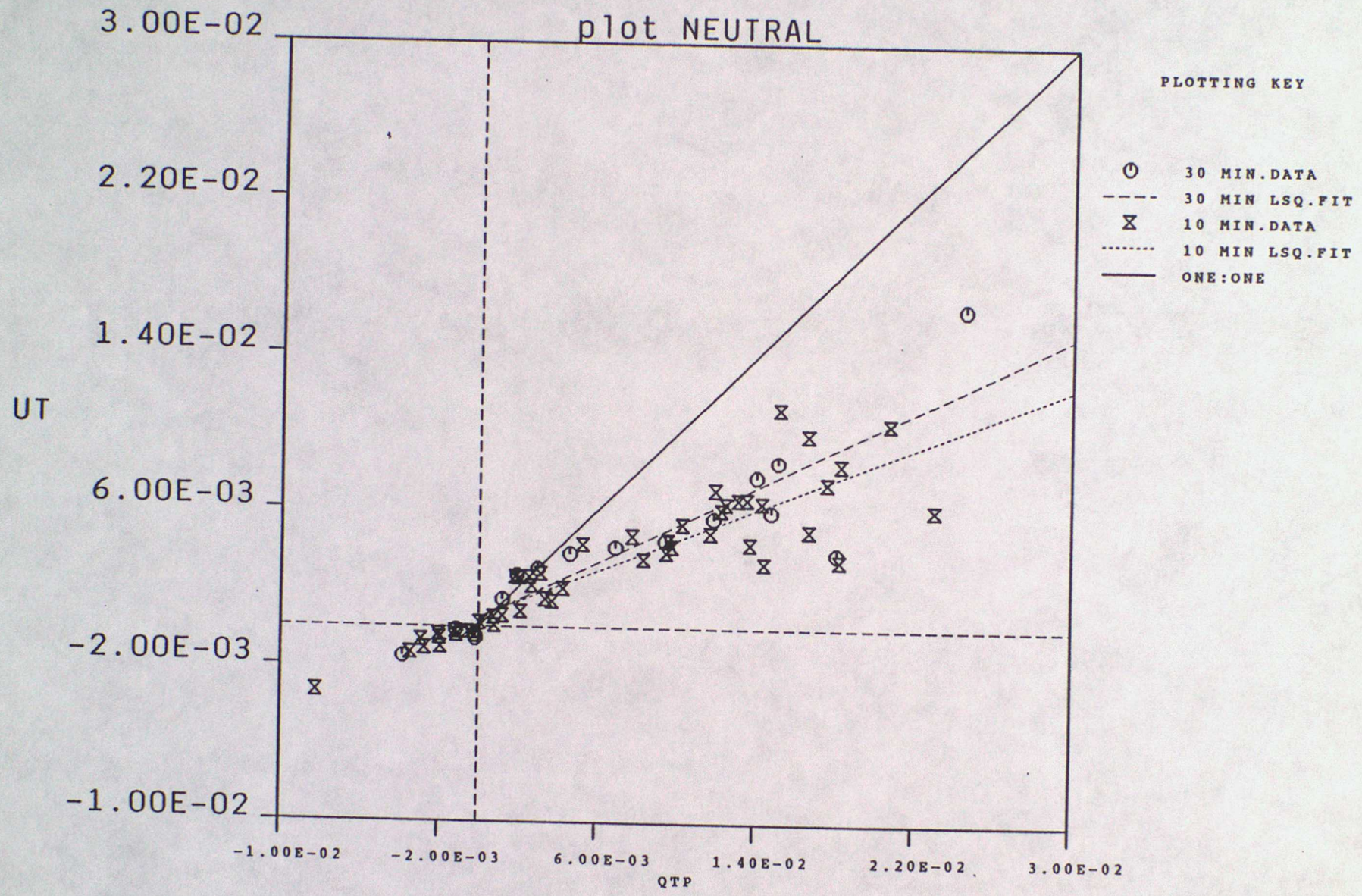
plot NEUTRAL
3.00E-02
2.20E-02
1.40E-02
6.00E-03
-2.00E-03
-1.00E-02
UT
-1.00E-02
-2.00E-03
6.00E-03
1.40E-02
2.20E-02
3.00E-02
QTP
PLOTTING KEY
30 MIN.DATA
30 MIN LSQ.FIT
10 MIN.DATA
10 MIN LSQ.FIT
ONE:ONE

FIGURE 8

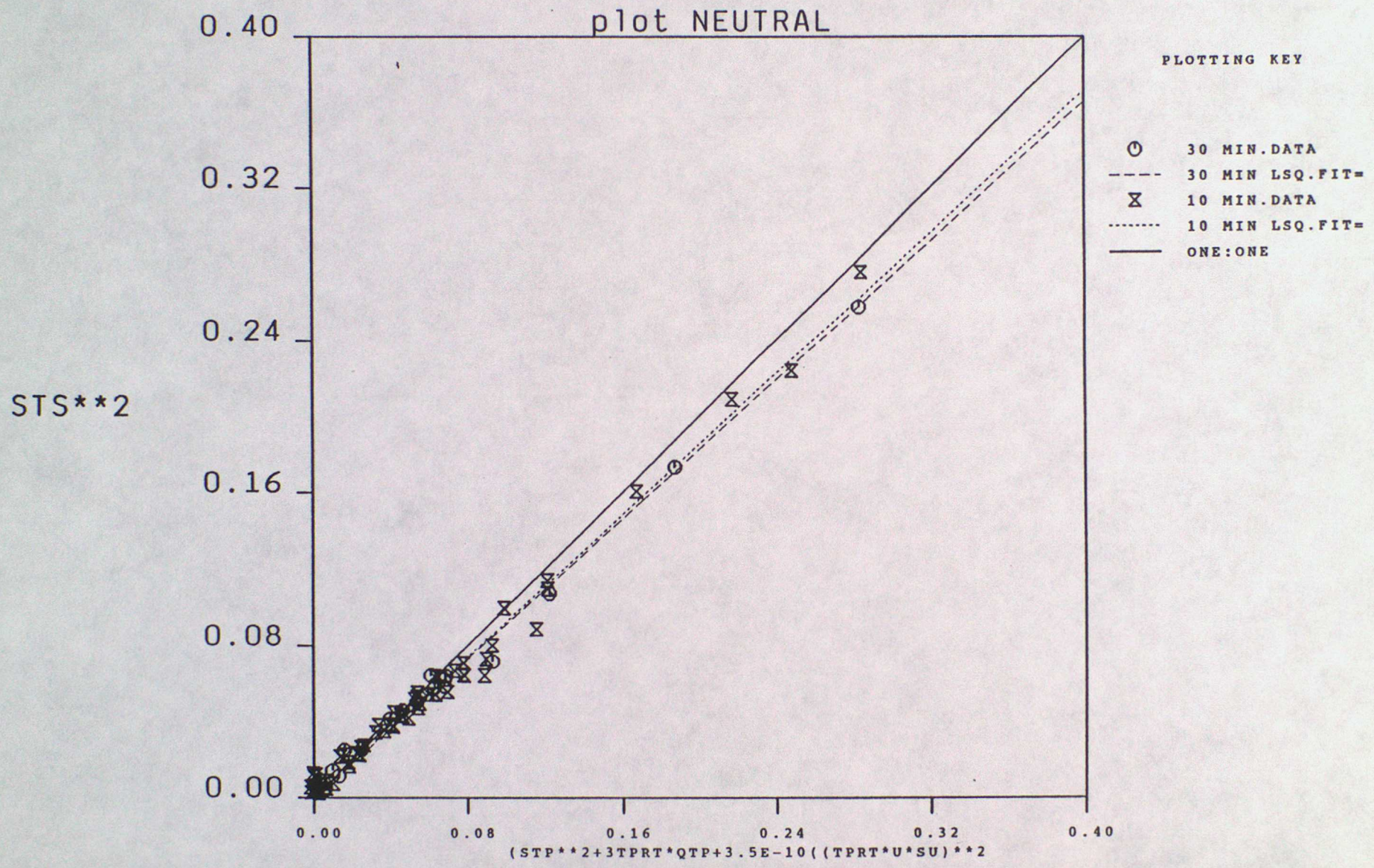
plot NEUTRAL
0.40
0.32
0.24
0.16
0.08
0.00
STS**2
0.00
0.08
0.16
0.24
0.32
0.40
(STP**2+3TPRT*QTP+3.5E-10((TPRT*U*SU)**2
PLOTTING KEY
30 MIN.DATA
30 MIN LSQ.FIT=
10 MIN.DATA
10 MIN LSQ.FIT=
ONE:ONE

FIGURE 9

use of equation (15) can once again be explained by accumulation effect of positive terms 2 to 4. The correction terms within (15) had relative magnitudes of 30%, 28%, 31%, 4%, 6% and a data spread equivalent to 90% spread of $\sigma^2_{T_s}$.

The errors involved during near neutral conditions (3%) were in general larger than those for unstable and stable conditions which can be explained for the unstable case due to a shift of spectral peaks at higher frequencies. An investigation carried out by Schotanus et al., 1983 indicated that for values of σ_{T_s} lower than 0·5 then the σ_{T_s} approx. terms $< \sigma_{T_s}$. This result has only been partly verified here since the data sets analysed had sonic temperature fluctuations only less than 0·5k and the paper adds that for $\sigma_{T_s} > 0 \cdot 5$ then neutral data was approximated by

$$\sigma^2_{T_s} \simeq \sigma^2_T + 1 \cdot 22\,\overline{T}\;\overline{q'T'} \tag{18}$$

However, the resulting σ_{T_s}, σ_T magnitude change from successive approximations may be explained by the consideration of the thermal response time of the platinum resistance thermometer which could have caused an error in the measured σ_T for this stability case.

Term 6 of relation (15) was found to have a negligible effect on fluctuations in sonic temperature under near neutral conditions.

4.1.3 Unstable

For a correlation which closely followed a one: one linear relationship, the first four correction terms from relation (11) were required, enabling for unstable conditions this relation to be reduced to (19) below

$$\sigma^2_{T_s} \simeq \sigma^2_T + 1 \cdot 22\;\overline{T}\;\overline{q'T'} + (0 \cdot 61)^2\,\overline{T}^2\sigma^2_q + \frac{4\overline{T}^2}{(\overline{c^2})^2}\,\overline{u}^2\sigma^2 u \tag{19}$$

This relation holds very well as shown by Figure 10 with values of σ_{T_s} on average 3% less than those of the approx σ_{T_s}. Initial approximations gave low gradient representations of a 6 - 10% variation from the theoretically derived relationship (11). Addition of successive corrections terms to the approximation produced a marked improvement though prevented from perfect correlation by the stated 3% variation. An investigation into the apparent negligibility of correction terms 5 and 6 contained within relation (11) resulted solely in the clarification that the magnitude of the terms, 2% and 1%

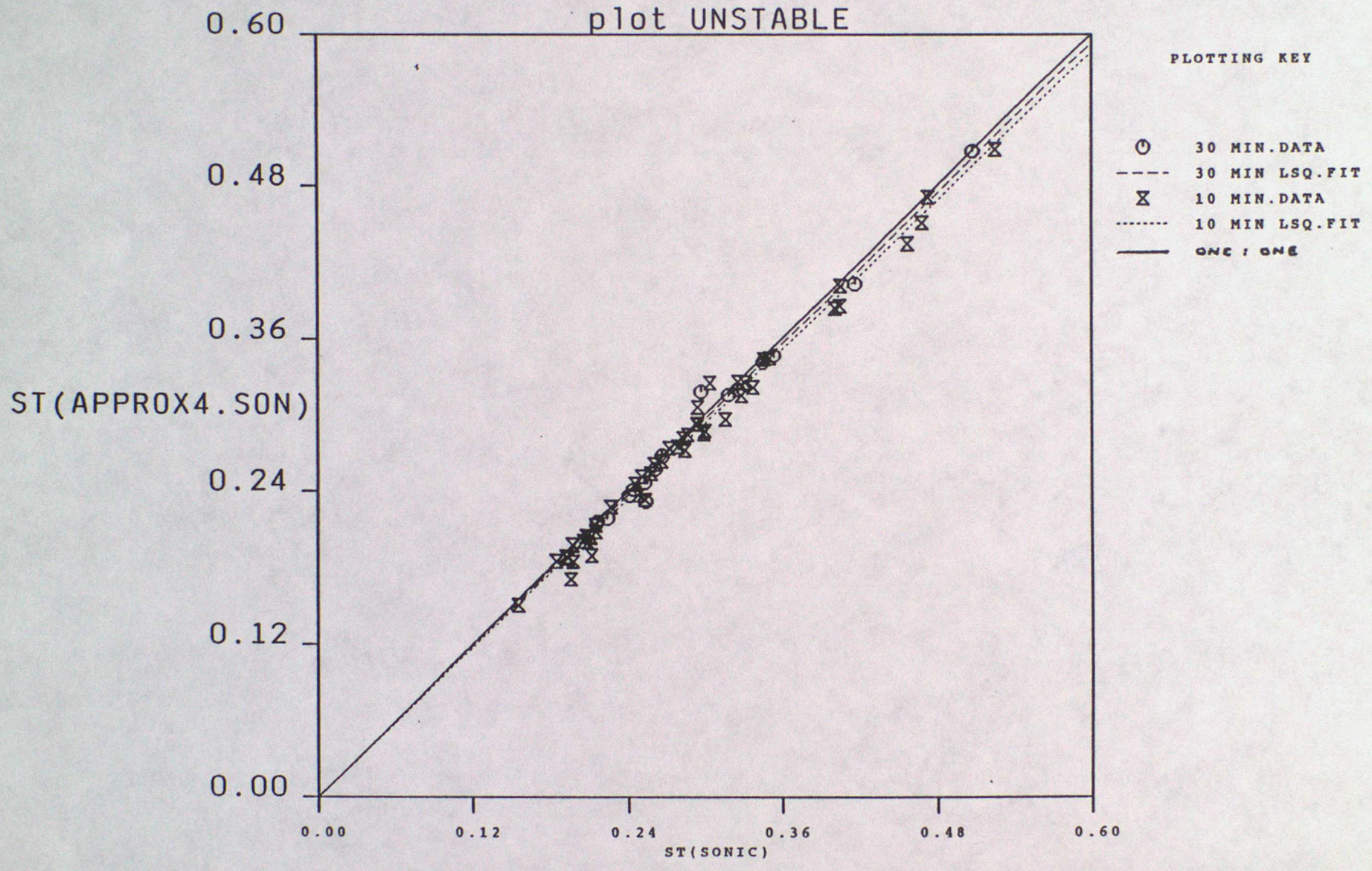
plot UNSTABLE
0.60
0.48
0.36
0.24
0.12
0.00
ST(APPROX4.SON)
0.00
0.12
0.24
0.36
0.48
0.60
ST(SONIC)
PLOTTING KEY
30 MIN.DATA
30 MIN LSQ.FIT
10 MIN.DATA
10 MIN LSQ.FIT
ONE : ONE

FIGURE 10

respectively, were insignificant and was not as a result of a relationship between any other parameters within the relation. The dominant term in relation (19) above was that of σ_T^2 which contributed 78% of magnitude of approximation with terms 2 and 3; 9% each. The σ_u^2 term though of only 2% magnitude was a justifiable correction as its ommitance produced a known deviation in the slope of 4%. For experimental conditions under which rough approximations to fluctuations in sonic and PRT temperatures may be made, ($\pm$ 5%) a further reduction in relation (11) is permitted leading to (16). Figure 11 verified this relationship with σ_T noticeably greater than σ_{T_s}. For both the improved and rough approximations to $\sigma_{T_s}^2$ in unstable conditions the spread of the σ_T^2 data was equivalent to $\frac{1}{4}$ spread of $\sigma_{T_s}^2$ data with a fractional contribution of the whole,from the first two terms of $\frac{4}{10}$ and $\frac{1}{4}$ respectively.

The attempt to realise any relationship between the mean terms had the conclusion that for unstable conditions the terms were effectively independent of each other.

The successive correlation improvement that occurred, as shown by Figure 12, resulted in an increase in the slope for each term other than fourth until it obtained a magnitude $> 1 \cdot 0$. The corrective fourth term had a 5% reduction effect which resulted in the significantly improved approximation (19).

4.2 Covariances

The covariance flux given by (12)) was next considered, to likewise deduce the degree of correlation for each atmospheric stability condition.

4.2.1 Stable

For stable conditions, successive approximations to the covariance flux were drawn. Analysis of the figures resulted in the reduction of relation (11) to (20) below

$$\overline{w'T_s'} = \overline{w'T'} \tag{20}$$

Figure 13 illustrated well the degree of correlation present between the two parameters. From direct calculation, it was observed that this simplified relation proved to be the closest to perfectly correlated data, of the three approximations, with a slope of 0·96. On average $\overline{w'T_s'}$ had a larger value than approx to $\overline{w'T_s'}$; 3% greater in magnitude.

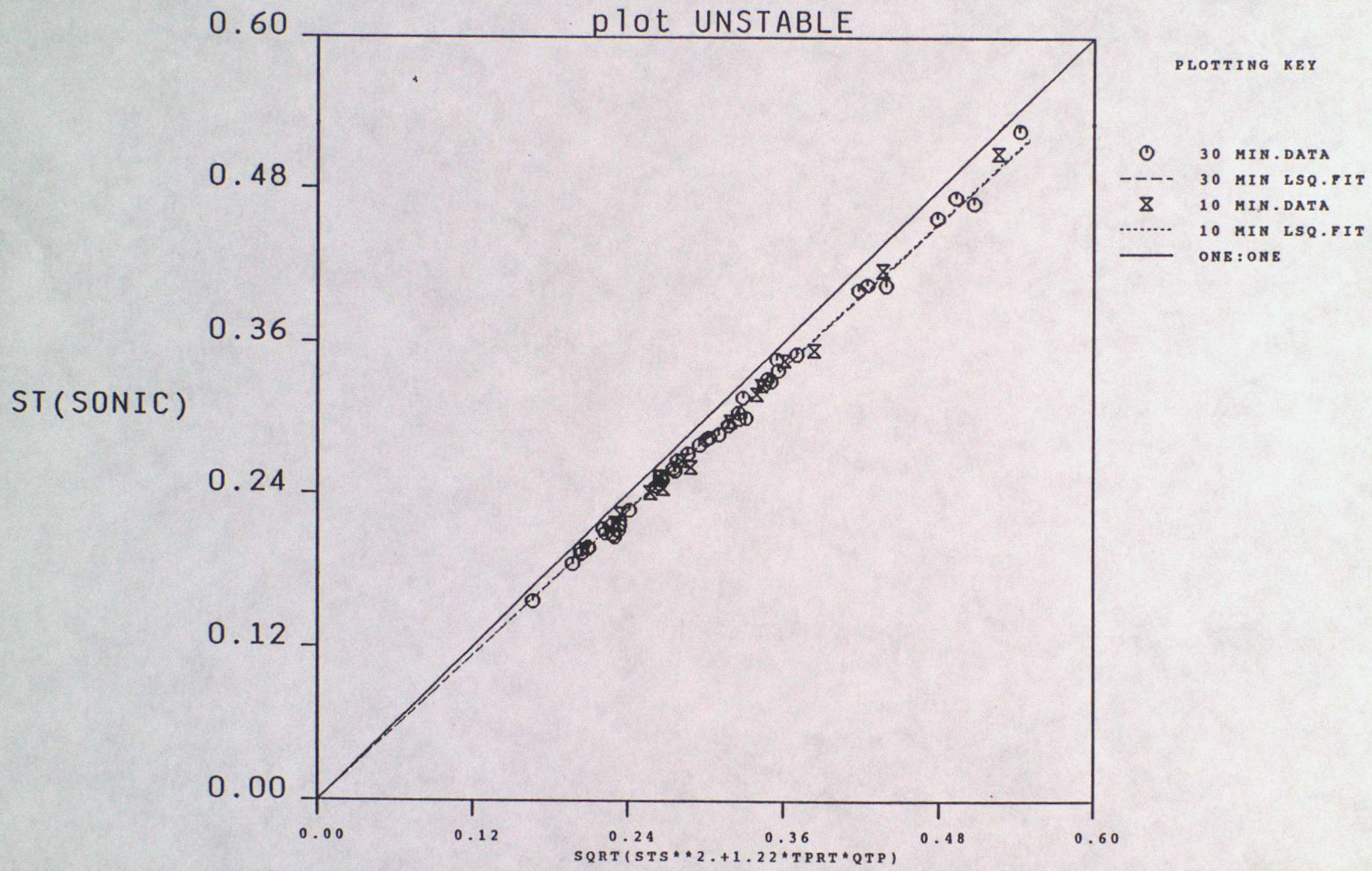
plot UNSTABLE
0.60
0.48
0.36
0.24
0.12
0.00
ST(SONIC)
0.00
0.12
0.24
0.36
0.48
0.60
SQRT(STS**2.+1.22*TPRT*QTP)
PLOTTING KEY
30 MIN.DATA
30 MIN LSQ.FIT
10 MIN.DATA
10 MIN LSQ.FIT
ONE:ONE

FIGURE 11

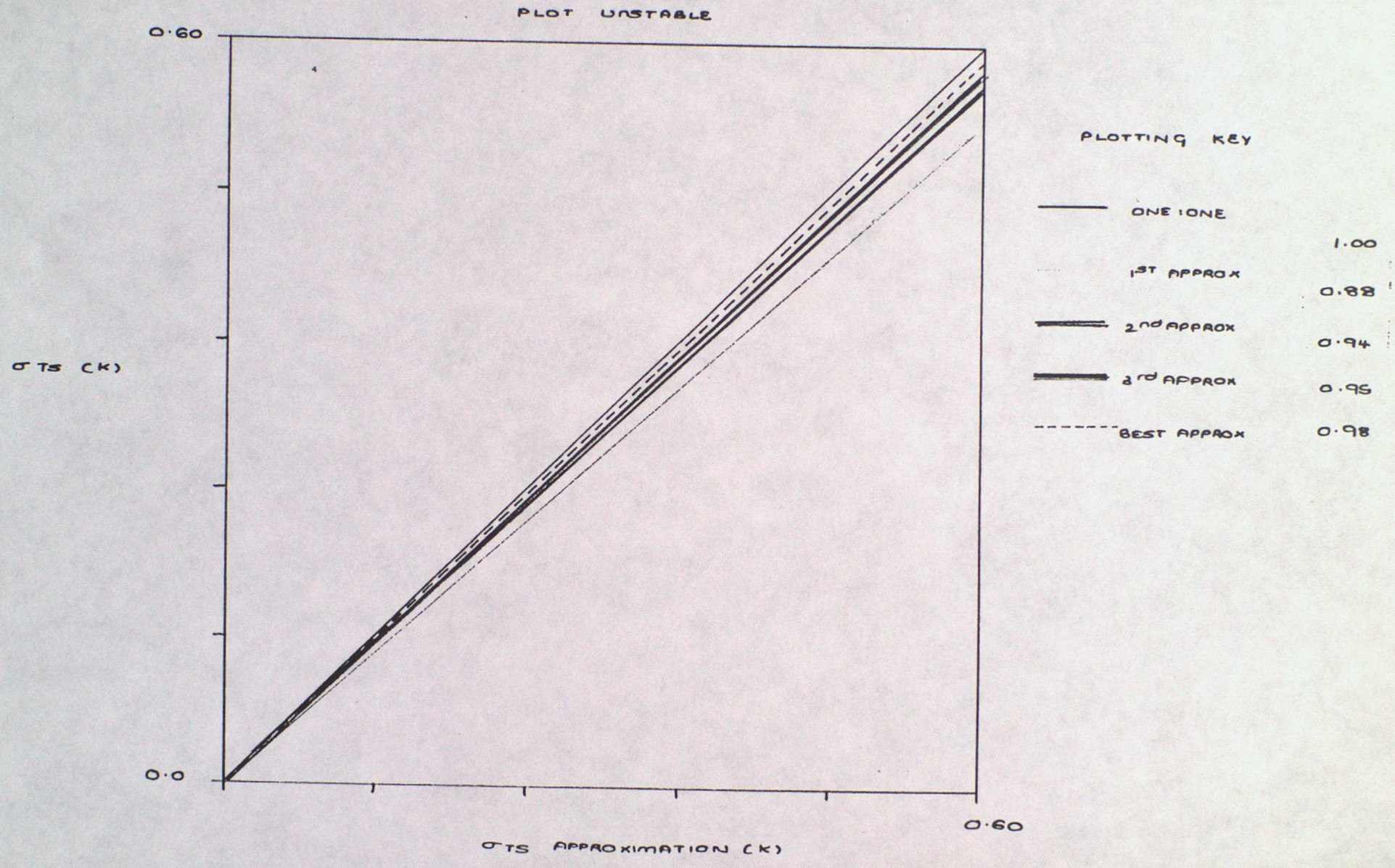
PLOT UNSTABLE
0·60
0·0
σ TS (K)
σ TS APPROXIMATION (K)
0·60
PLOTTING KEY
ONE : ONE
1·00
1ST APPROX
0·88
2nd APPROX
0·94
3rd APPROX
0·95
BEST APPROX
0·98

FIGURE 12

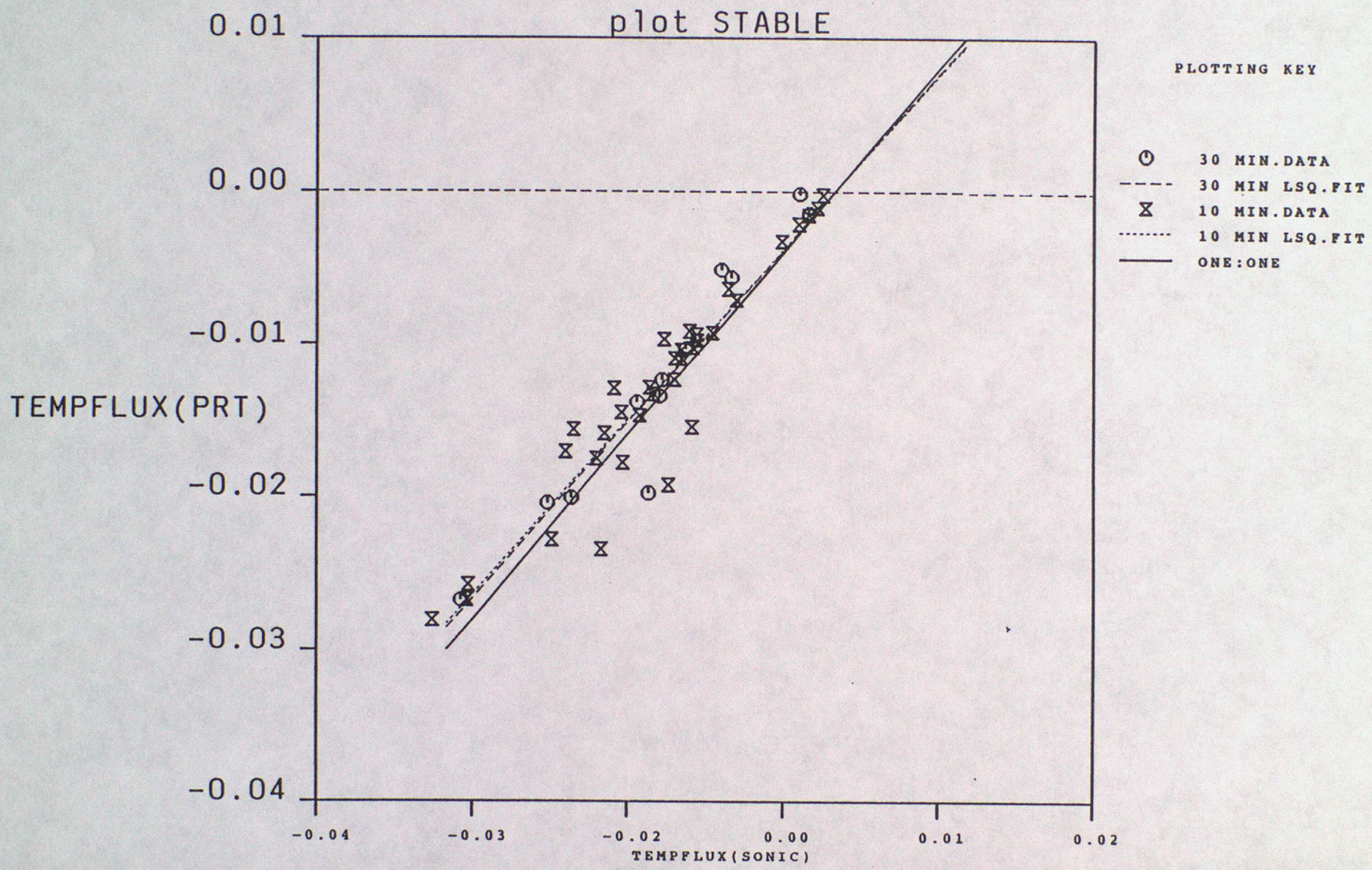
plot STABLE
0.01
0.00
-0.01
-0.02
-0.03
-0.04
TEMPFLUX(PRT)
-0.04
-0.03
-0.02
0.00
0.01
0.02
TEMPFLUX(SONIC)
PLOTTING KEY
30 MIN.DATA
30 MIN LSQ.FIT
10 MIN.DATA
10 MIN LSQ.FIT
ONE:ONE

FIGURE 13

In addition to (20) above an investigation of correlations contained within (21) and (22) below were also undertaken

$$\overline{w'T'}_s = \overline{w'T'} + 0 \cdot 61\,\overline{T}\;\overline{w'q'} \tag{21}$$

$$\overline{w'T'}_s = \overline{w'T'} + 0 \cdot 61\,\overline{T}\;\overline{w'q'}\;\frac{-2}{\overline{c^2}}\;\overline{T}\,\overline{u}\,\overline{u'w'} \tag{22}$$

Graphical analysis led to the result that for stable conditions as the number of correction terms contained within the sonic heat flux increased, relation (11), so did the degree of deviation from true one: one linear relationships. The successive deviations brought about by each term being represented by Figure 14.

For relation (20) the ignored $\overline{w'q'}$ and $\overline{u'w'}$ correction terms were found to have a slight effect on the overall relation only, contributing relative magnitudes - in comparison to the whole relation - of 5% and 3% respectively. The successive correction terms had in addition % spread distributions of 65%, 25% and 6·5%.

The third approximation by the inclusion of the $\overline{u'w'}$ term caused a slope deviation of 12% though the term had only a 3% effect on correction terms 1 and 2.

The relative order of importance of terms is given by the order of the terms in (11), with regards to their magnitude and spread, with $\overline{w'T'}$ the greatest contributing factor. These findings show that under stable conditions the measured sonic covariance heat flux is equivalent to the PRT covariance heat flux. Determination of an explanation as to the reason why terms 2 and 3 were insignificant under stable conditions was undertaken by the correlation of moisture flux ($\overline{w'q'}$) and momentum flux ($\overline{u'w'}$) to observe if any relationship existed which was producing an effective cancellation of the terms.

As a result, the latter two terms vary the relation little as their magnitude were small.

Both 10 and 30 minute averaged data was employed for the analysis and it was found that there was no real significant difference between the values of the two averaged - timed sets.

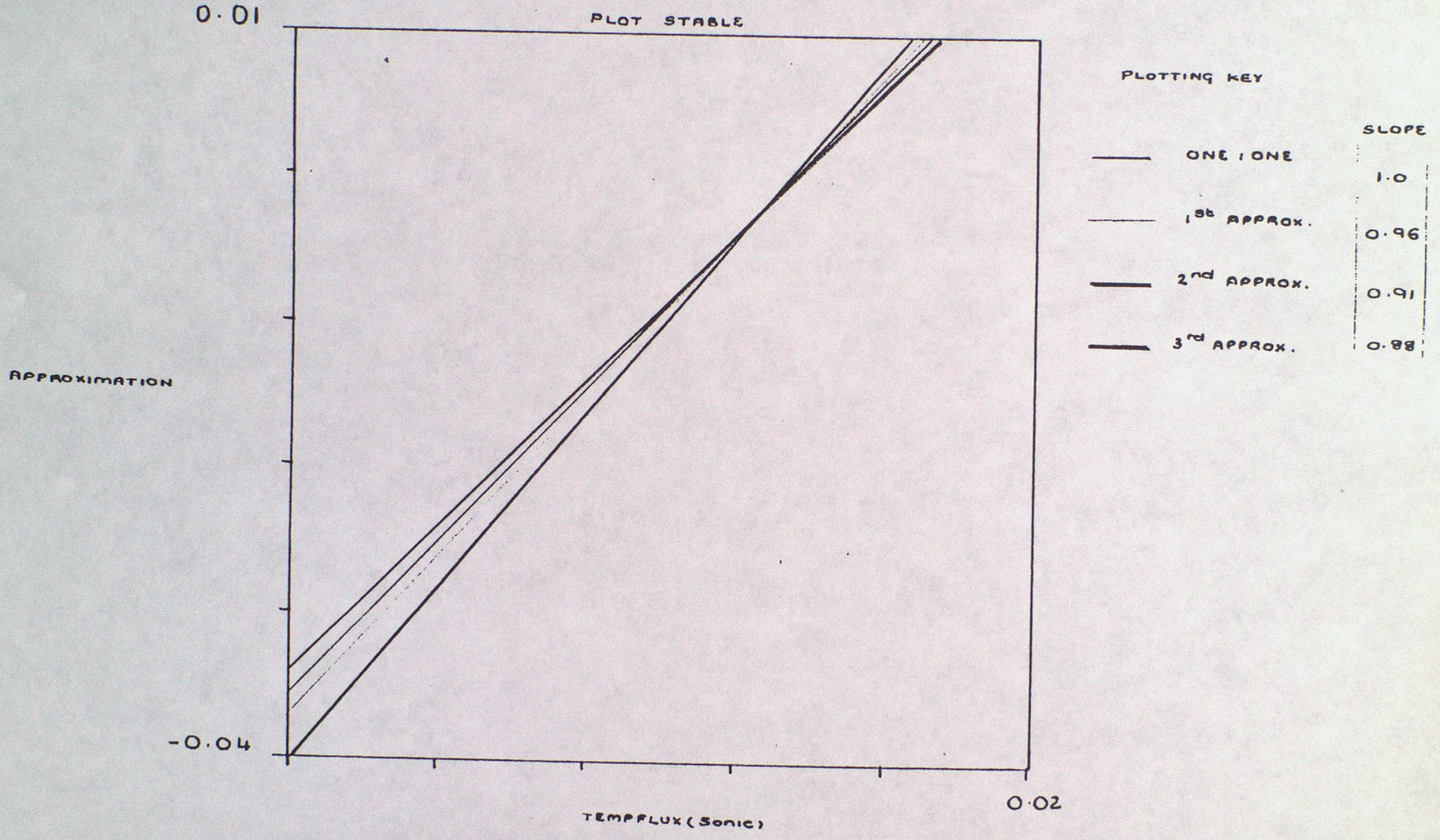
0.01
PLOT STABLE
APPROXIMATION
-0.04
0.02
TEMPFLUX (Sonic)
PLOTTING KEY
SLOPE
ONE : ONE
1.0
1st APPROX.
0.96
2nd APPROX.
0.91
3rd APPROX.
0.88

FIGURE 14

4.2.2 Neutral

Under the stability range of nearly neutral conditions a more complicated relation was required, to obtain a sufficient correlation of $\overline{w'T'_s}$ and $\overline{w'T'}$. This involved the addition of all three approximations, as in equation (11), which for the data gathered provided the best approximation.

$$\overline{w'T'}_s = \overline{w'T'} + 0 \cdot 61\ \overline{T}\ \overline{w'q'} - \frac{2}{\overline{c^2}}\ \overline{T}\,\overline{u}\ \overline{u'w'} \tag{23}$$

This approximation correlated well and is illustrated in Figure 15. On average $\overline{w'T'}_s$ was equivalent to the RHS of equation (11) with a deviation of only 1% from perfect slope calculation.

A study of the % importance of each term resulted in contributions of 80%,18%, 2% for terms 1 to 3 respectively though the spread of the relationship was dominated by the latter two correction terms each contributing 40%

As the addition of correction terms plotted against the sonic heat flux covariance successively increased a marked improvement in the degree to which the theoretical one: one relationship was obeyed occured.

Figure 16 shows this graphically with the correlation of $\overline{w'T'_s}$ against $\overline{w'T'}$ significantly worse than that for stable stability.

Analysis of relation (11) for nearly neutral conditions revealed that the moisture flux was an important correction term when combined with the PRT heat flux in order for a reasonable approximation to sonic heat flux to be made. Though this property was not as distinct in stable and unstable conditions.

For nearly neutral data, the RHS was a poor approximation to sonic covariance heat flux of equation (20)

$$\overline{w'T'}_s = \overline{w'T'} \tag{24}$$

with $\overline{w'T'}$ contribution of 80% the magnitude of $\overline{w'T'}$ and an error of 40% in the slope determination an indication of the significance of the omitted terms of relation (11) is given. In theory, neutral stability occurs when there is a zero heat flux.

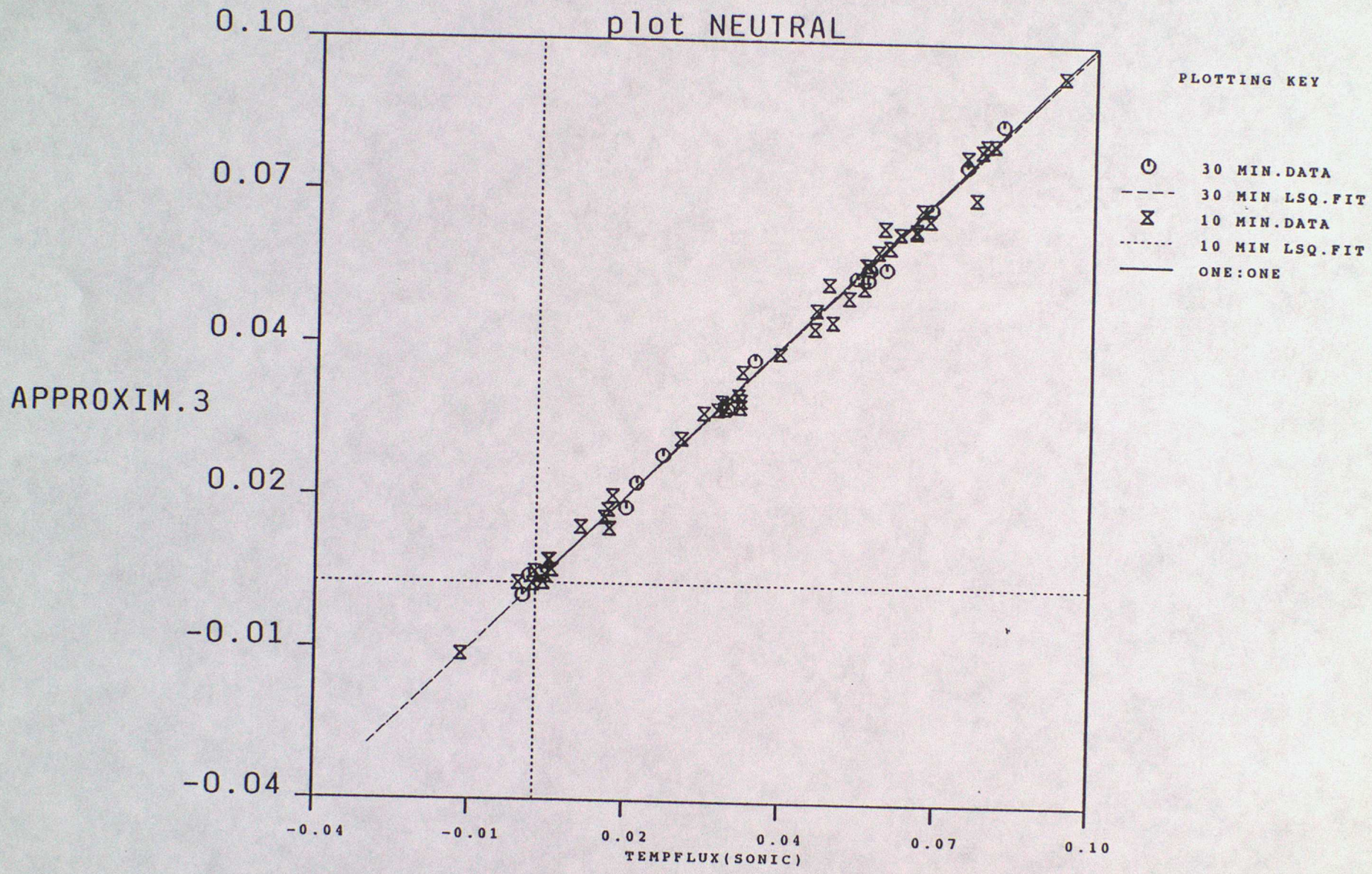
plot NEUTRAL
0.10
0.07
0.04
APPROXIM.3
0.02
-0.01
-0.04
-0.04
-0.01
0.02
0.04
0.07
0.10
TEMPFLUX(SONIC)
PLOTTING KEY
30 MIN.DATA
30 MIN LSQ.FIT
10 MIN.DATA
10 MIN LSQ.FIT
ONE:ONE

FIGURE 15

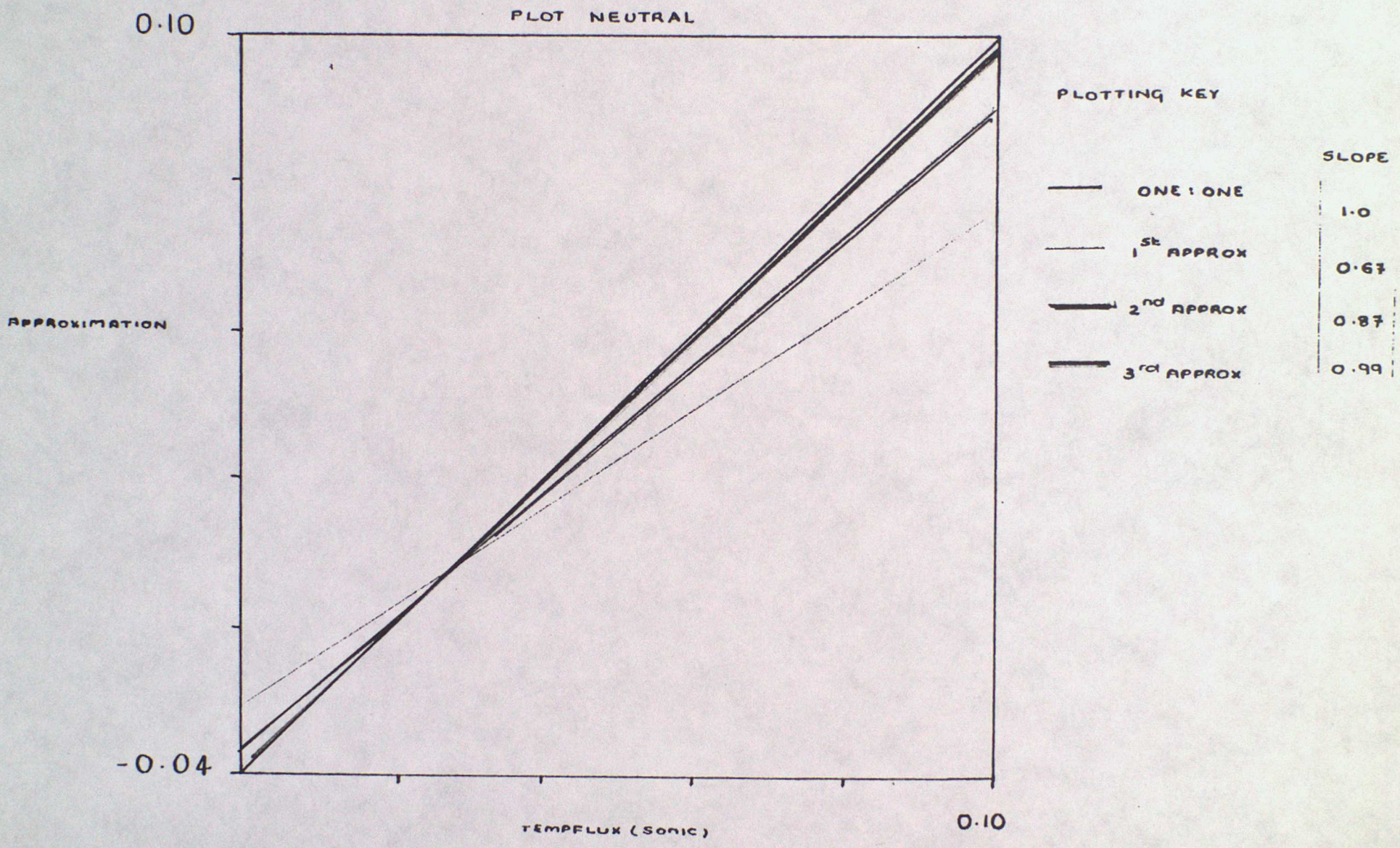
PLOT NEUTRAL
0·10
-0·04
APPROXIMATION
TEMPFLUX (SONIC)
0.10
PLOTTING KEY
SLOPE
ONE : ONE
1·0
1st APPROX
0·67
2nd APPROX
0·87
3rd APPROX
0·99

FIGURE 16

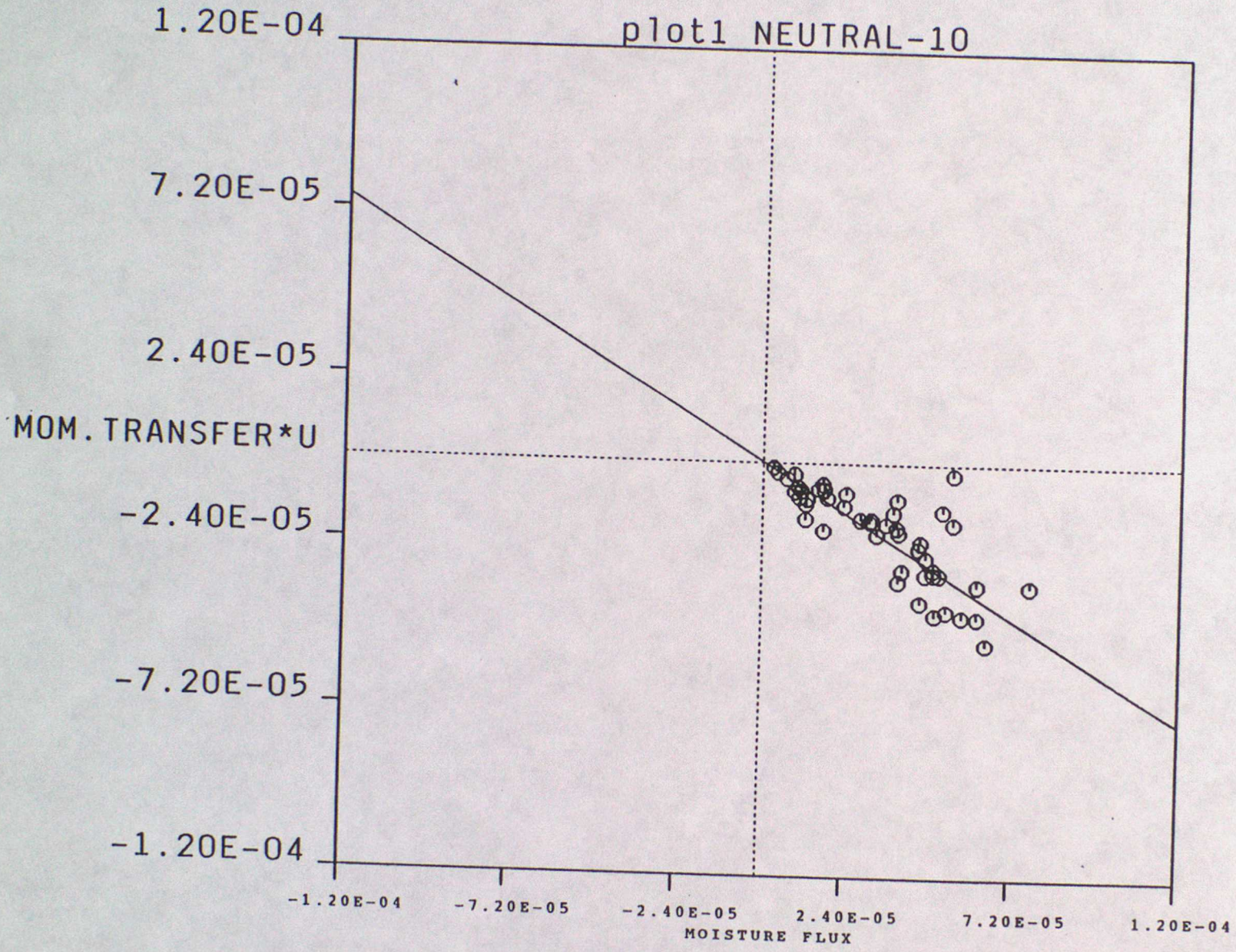
plot1 NEUTRAL-10
1.20E-04
7.20E-05
2.40E-05
MOM.TRANSFER*U
-2.40E-05
-7.20E-05
-1.20E-04
-1.20E-04
-7.20E-05
-2.40E-05
2.40E-05
7.20E-05
1.20E-04
MOISTURE FLUX

FIGURE 17

The second approximation improved the correlation rapidly due to the significant $\overline{w'q'}$ term causing a reduction in the gradient error to 13%, though the relation involving all three terms was by far the best correlation.

The possible correlation of $\overline{w'q'}$ and $\overline{u'w'}$ was considered similarly for nearly neutral data. Figure 17 shows the negative gradient relationship. Though the trend was limited due to the small magnitude of the plots and the presence of data scatter a correlation between moisture flux and momentum flux was apparent though its exact magnitude was difficult to observe.

4.2.3 Unstable

The best approximation to unstable conditions involved all three terms of the sonic covariance heat flux relation (11), given below.

$$\overline{w'T'}_s = \overline{w'T'} + 0 \cdot 61\ \overline{T}\,\overline{w'q'} - \frac{2}{c^2}\,\overline{T}\,\overline{u}\,\overline{u'w'} \tag{25}$$

which varied from perfect one: one correlation by 3%. This best approximation to unstable conditions, Figure 18, can be seen to obey the theoretical relation extremely well. From Figure 18, on average the three termed approximation to $\overline{w'T'}_s > \overline{w'T'}_s$.

As means of a comparison additional analysis of the further two approximations were made. A graphical investigation resulted in the conclusion that for unstable conditions, as the correction terms added to PRT covariance heat flux increases so does the correlation with the sonic heat flux. An illustration of this is given by Figure 19.

The three flux terms contained within (11) were found to contribute varying relative magnitudes with PRT temperature flux the major contributor - 93% with % magnitude of moisture flux and momentum flux 4% and 3% respectively. Though, the spread of each term was large compared to the two further stability conditions, of 47%, 32% and 21%.

Determination of whether the momentum flux was related to the humidity flux produced a large data scatter so no relationship could be defined under unstable conditions.

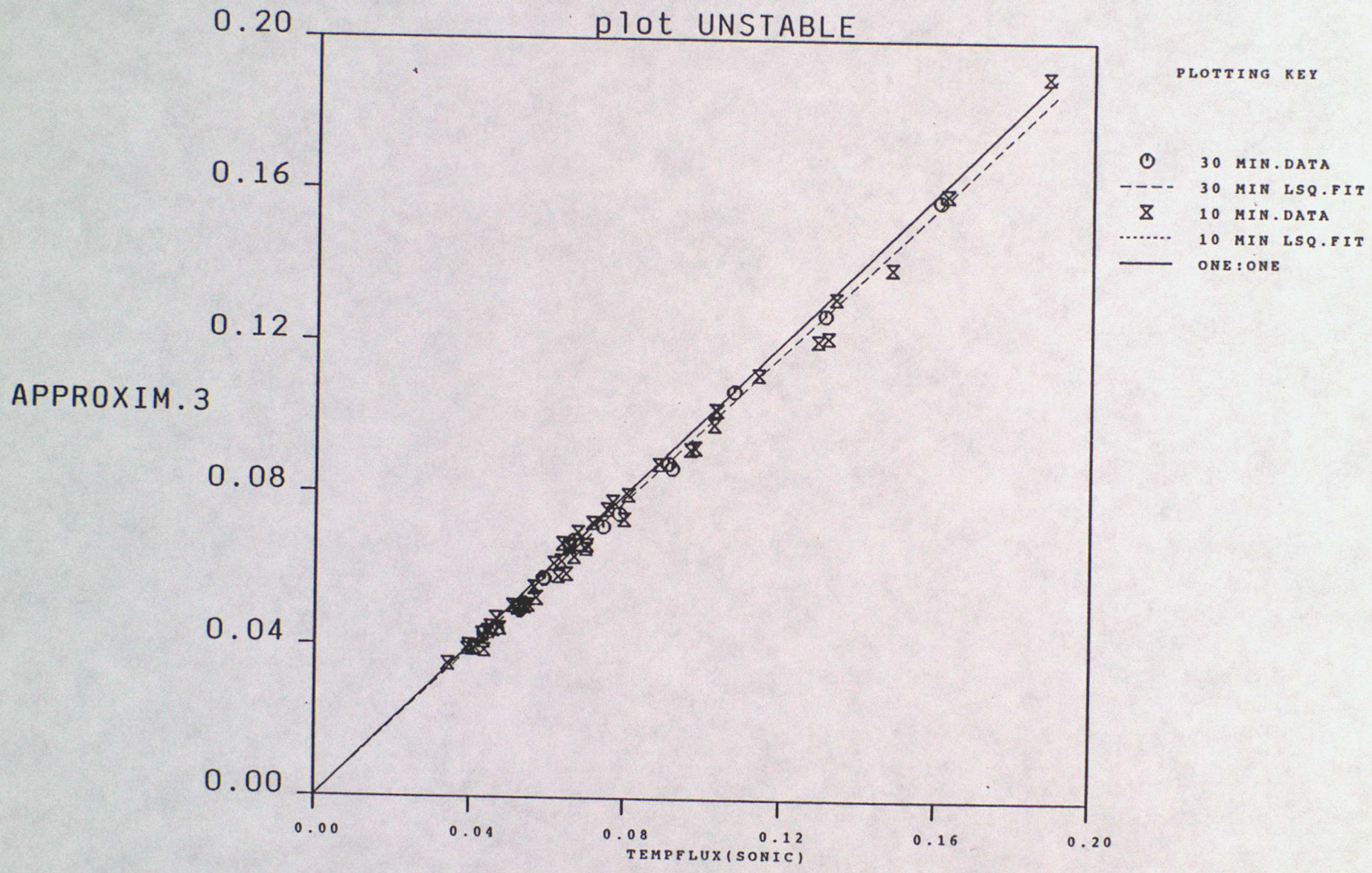
plot UNSTABLE
APPROXIM.3
0.20
0.16
0.12
0.08
0.04
0.00
0.00
0.04
0.08
0.12
0.16
0.20
TEMPFLUX(SONIC)
PLOTTING KEY
30 MIN.DATA
30 MIN LSQ.FIT
10 MIN.DATA
10 MIN LSQ.FIT
ONE:ONE

FIGURE 18

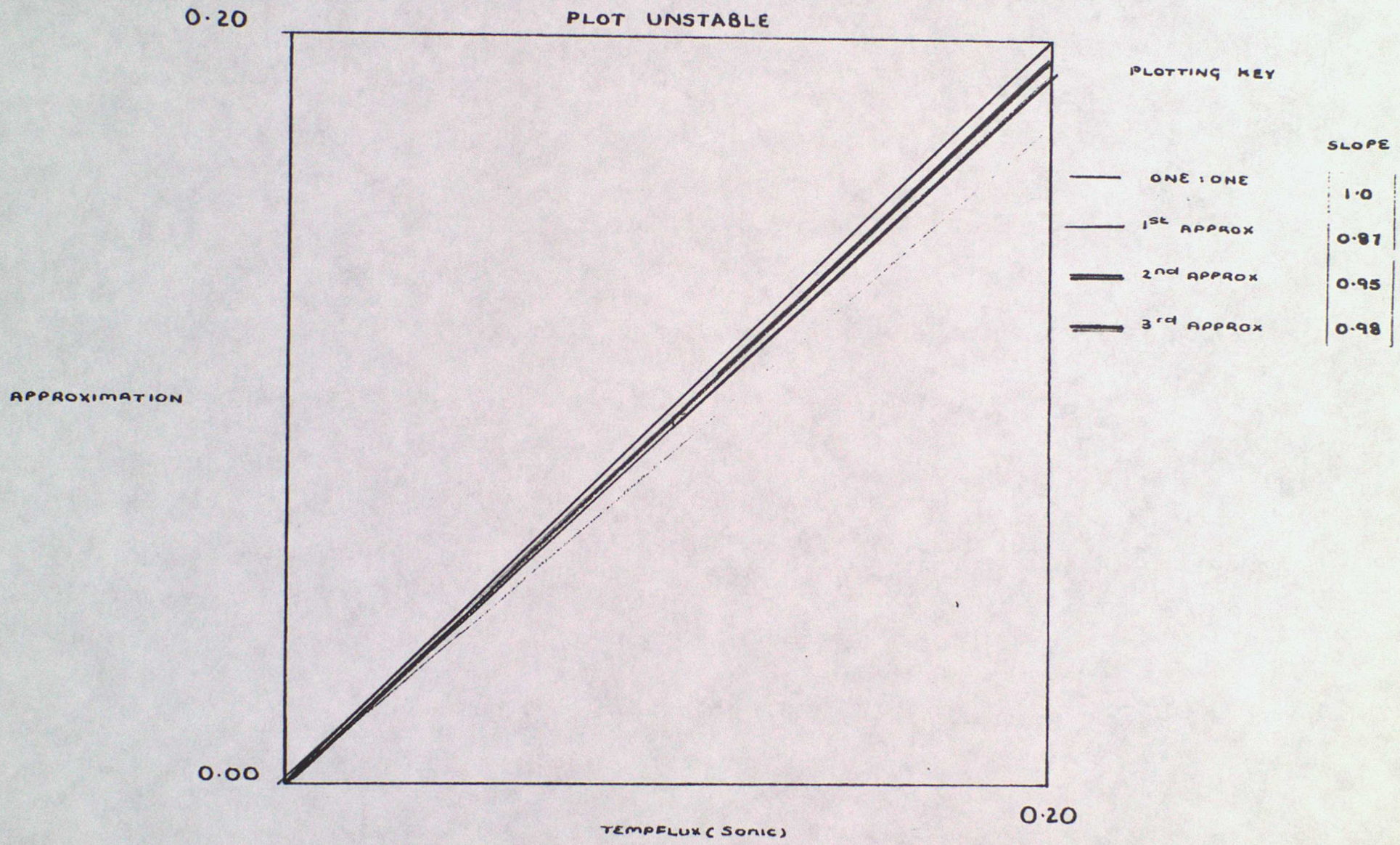
0·20
PLOT UNSTABLE
PLOTTING KEY
SLOPE
ONE : ONE
1·0
1ST APPROX
0·97
2ND APPROX
0·95
3RD APPROX
0·98
APPROXIMATION
0·00
0·20
TEMPFLUX (Sonic)

FIGURE 19

5 Conclusions

Simultaneous measurements from a sonic anemometer, platinum resistance thermometer and an IR-hygrometer were presented. A brief review of sonic anemometer theory for temperature calculations was carried out along with the derivation of expressions for the sonic anemometer temperature variance and heat flux for stable, nearly neutral and unstable turbulence conditions. With the aid of direct measurements of temperature and humidity fluctuations the degree of departure from the derived relations for each stability range was determined along with the best simplified relation for an accurate correlation. The following results were obtained.

5.1 Stable

1. Sonic temperature fluctuations are equivalent to PRT temperature fluctuations to within $\sim 2°$

$$\sigma T_s \simeq \sigma_T \tag{26}$$

2. Best approximation to covariance heatflux.

   Rough approximation 92% accuracy

$$\overline{w'T's} = \overline{w'T'} \tag{27}$$

   Improved approximation 97% accuracy

$$\overline{w'T'}_s = \overline{w'T'} + 0 \cdot 61\, \overline{T}\, \overline{w'q'} \tag{28}$$

5.2 Neutral

Further complex correction terms are required to achieve good correlations, than for stable and unstable conditions.

1. Sonic temperature fluctuations can be approximated by:

$$\sigma^2 T_s = \sigma^2 T + 1 \cdot 22\ \overline{T}\,\overline{q'T'} + (0 \cdot 61)^2\,\overline{T}^2\,\sigma^2 q + \frac{4\overline{T}^2}{(\overline{c^2})^2}\,\overline{u}^2\sigma^2 u \qquad (29)$$

$$-\frac{4\overline{T}}{\overline{c^2}}\,\overline{u}\,\overline{u'T'}$$

2. Covariance sonic heat flux relation for neutral data

$$\overline{w'T'_s} = \overline{w'T'} + 0 \cdot 61\ \overline{T}\ \overline{w'q'} - \frac{2}{\overline{c^2}}\,\overline{T}\,\overline{u}\,\overline{u'w'} \qquad (30)$$

98% accuracy

5.3 Unstable

1. Variance of sonic temperature fluctuations correlation

$$\sigma^2 T_s = \sigma^2 T + 1 \cdot 22\ \overline{T}\ \overline{q'T'} + (0 \cdot 61)^2\,\overline{T}^2\sigma^2 q \qquad (31)$$

$$+\frac{4}{\overline{c^2}}\,\overline{T}^2\,\overline{u}^2\sigma^2 u$$

2. covariance sonic heat flux relation.

$$\overline{w'T'_s} = \overline{w'T'} + 0 \cdot 61\ \overline{T}\ \overline{w'q'}\ \frac{-2}{\overline{c^2}}\ \overline{T}\,\overline{u}\,\overline{u'w'} \qquad (32)$$

97% accuracy

Acknowledgements

I am very grateful for the staff at the Meteorological Research Unit, Cardington, Bedford for their help during this report and the technical set-up of the measuring instruments, and in particular to Mrs G Kimpton for her painstaking care in typing the manuscript.

References

Kaimal, J.C. and Businger, J.A., 1963 "A continuous - wave sonic anemometer - thermometer"; J. Appl. Meteorol. 2, 156-164

Kaimal, J.C., 1969, "Measurement of momentum and heat flux variations in the surface boundary layer" Radio Science 4, 1147-1153

Schotanus, P., Nieuwstadt, F.T.M., Debruin, H.A.R., 1983 "Temperature measurement with a sonic anemometer and its application to heat and moisture fluxes"; Boundary Layer Meteor., 26, 81-93

Appendix

Appendix A

$$(1/t_1 + 1/t_2) = (\frac{2c\cos\alpha}{L})$$

(A1)

The sound velocity is given by:

$$c^2 = \gamma RT(1 + 0 \cdot 61q)$$

(A2)

$$(1/t_1 = 1/t_2)^2 = \frac{4c^2\cos^2\alpha}{L^2}$$

(A3)

$$(1/t_1 + 1/t_2)^2 = \frac{4\gamma RT(1 + 0 \cdot 61q)\cos^2\alpha}{L^2}$$

(A4)

$$T = T_s$$

(A5)

$$T_s = \frac{L^2}{4\gamma R}\{\frac{1}{t_1} + \frac{1}{t_2}\}^2$$

(A6)

Appendix B

(A6) becomes:

$$T_s = \frac{L^2}{4\gamma R}\left(\frac{4c^2\cos^2\alpha}{L^2}\right)^2 \tag{B1}$$

$$T_s = \frac{c^2}{\gamma R}\cos^2\alpha \tag{B2}$$

$$T_s = T(1 + 0\cdot 61q)\cos^2\alpha \tag{B3}$$

$$T_s = T(1 + 0\cdot 61q) \tag{B4}$$

from mean and fluctuating parts of terms given by (s)

$$T_s = (\overline{T} + T')(1 + 0\cdot 61\,\overline{q} + 0\cdot 61q')(\overline{\cos\alpha} + \cos\alpha')^2 \tag{B5}$$

but

$$\cos^2\alpha = \left(1 - \frac{vn^2}{c^2}\right) = \left(1 - \frac{vn^2}{(\bar{c}+c')^2}\right) \tag{B6}$$

$$T_s = \overline{T}\ \overline{\cos^2\alpha} + 2\,\overline{T}\,\overline{\cos\alpha}\,\cos\alpha' + 0\cdot 61\ \overline{q}\overline{T}\,\overline{\cos^2\alpha}$$

$$+ 2\,x\,0\cdot 61\ \overline{q}\,\overline{T}\overline{\cos\alpha}\cos\alpha' + 0\cdot 61\,x\,2\ \overline{T}q'\overline{\cos\alpha}\cos\alpha'$$

$$+T'\,\overline{\cos^2\alpha} + 2\,T'\,\overline{\cos\alpha}\cos\alpha' + 0\cdot 61\,T\,\overline{q}\overline{\cos^2\alpha}$$

$$+ 2\,x\,0\cdot 61\,T'\,\overline{q}\ \overline{\cos\alpha}\ \cos\alpha' + 0\cdot 61\,q'\,T'\cos^2\alpha + 2\,x\,0\cdot 61q'T'x\,\overline{\cos\alpha}\cos\alpha'$$

(B7)

but

$$T_s = \overline{T_s} + T_s'$$

(B8)

for

$$\overline{T_s} = \overline{T}\ \overline{\cos^2\alpha} + 0\cdot 61\,\overline{q}\,\overline{T}\ \overline{\cos^2\alpha}$$

(B9)

$$\overline{T_s} = \overline{T}(1 + 0\cdot 61\,\overline{q})$$

(B10)

From the remaining terms and substitution

$$T_s' = T' + 0\cdot 61q'\overline{T} - \frac{2\overline{T}}{c^2}\ \overline{vn}\ vn'$$

(B11)

Appendix C

Calculation of the variance of T

$$T_s' = T' + 0\cdot 61\,q'\ \overline{T}\ - \frac{2\overline{T}}{c^2}\ \overline{v_n}\,v_n'$$

(C1)

$$\sigma^2 T_s \equiv \overline{T'^2_s} = (T' + 0 \cdot 61\, q' \overline{T} - \frac{2\overline{T}}{c^2}\, \overline{v_n} v'_n)^2$$

(C2)

$$\sigma^2 T_s = T'^2 + 2\,x\,0 \cdot 61\, q' \overline{T} T' - 2T' \overline{T}\, \overline{v_n}\, v'_n$$
$$+ (o \cdot 61)^2\, q'^2\, \overline{T}^2 - \frac{2\,x\,0 \cdot 61}{c^2}\, q' \overline{T}^2 \overline{v_n}\, v'_n$$
$$- \frac{4}{c^2} T' \overline{T}\, \overline{v_n}\, v'_n - \frac{2\,x\,0 \cdot 61}{c^2}\, \overline{T}^2\, \overline{v_n}\, v'_n\, q'$$
$$+ \frac{4}{c^4} \overline{T}^2\, \overline{v_n}^2\, v'^2_n$$

(C3)

but

$$v_n = u$$

(C4)

variance

$$\sigma T^2 = \Sigma\, (T - \overline{T})^2 = \Sigma\, (T')^2$$

(C5)

$$T'^2 = \sigma\, T^2$$

(C6)

also

$$q'^2 = \sigma q^2$$

(C7)

$$u'^2 = \sigma u^2$$

(C8)

so

$$\sigma^2 T_s = \sigma^2 T + 1 \cdot 22\, \overline{T}\, \overline{q'T'} + 4 \frac{\overline{T}^2\, \overline{u}^2}{(c^2)^2}\, \sigma u^2$$
$$+ (0 \cdot 61)^2\, \overline{T}^2\, \sigma^2 q - 4 \frac{\overline{T}\, \overline{u}}{c^2}\, \overline{u'T'} - 2 \cdot 44 \frac{\overline{T}}{c^2}^2 \overline{u}\, \overline{u'q'}$$

(C9)

Appendix D

Covariance, correlation of T_s with the vertical velocity w

$$\overline{w'T_s'} = w'(T' + 0 \cdot 61 q' \overline{T} - \frac{2\,\overline{T}}{c^2}\,\overline{v_n} v_n') \tag{D1}$$

$$= w'T' + 0 \cdot 61\, w'\, q' \overline{T} - \frac{2w'}{c^2}\,\overline{T}\,\overline{v_n}\, v_n' \tag{D2}$$

$v_n = u$ and by taking means over all factors (w, T, q, u)

$$\overline{w'T_s'} = \overline{w'T'} + 0 \cdot 61\, \overline{w'q'}\,\overline{T} - \frac{2\overline{T}}{c^2}\,\overline{u}\,\overline{w'u'} \tag{D3}$$